Heritage Science

RESEARCH

Open Access

The sacrificial record in burial pits of the late Shang Dynasty: evidences from the chroma and magnetic properties of the Sanxingdui site, Sichuan, China

Yuming Guo[1], Fang Xiang[2,3*], Honglin Ran[4], Zhenbin Xie[4], Qi Yang[1], Hengxu Huang[3] and Li Ding[1]

Abstract

The Sanxingdui site (4.4–2.9 ka B.P.) in southwestern China is considered one of the most significant archaeological discoveries of the twentieth century, which contains numerous codes for interpreting the origin and development of the Yangtze River civilization. Remains found in Sanxingdui burial pits are keys to deciphering some of these codes. From the characters of the charcoal fragments, ashes and jades in the Sanxingdui buried pits, at the same time, comprehensively analyzing archaeological evidence and previous research results, we speculate that the temperature of ancient Shu people burning sacrifices could be 600–800 ℃. However, the values of magnetic properties and chroma of soils near the ash layers in the pits, and Guanghan Clay near the pits, do not show obvious changes caused by such high-temperature annealing. Combined with the geographical location of the pits and the accumulation characteristics of ash layers and artifacts in the pits, we consider that the Sanxingdui burial pits were not trash pits but sacrificial pits, and they were used for burying sacrifice after burning sacrifice. Although the ritual of burying sacrifice after burning sacrifice dates back to the Longshan period (4.3–4.0 ka B.P.) in China's Central Plain, the Sanxingdui sacrificial pits, which began to occur in the late Shang Dynasty (~ 3.0 ka B.P.) with such a large scale, and the sacrifices unearthed from the pits, are unique. So, we believe that although influenced by the Central Plain culture, the ancient Shu people in the late Shang Dynasty have unique characteristics of culture and religion.

Keywords Chroma, Magnetic properties, Burying sacrifice after burning sacrifice, Burial pit, The Sanxingdui site

Introduction

As one of the most remarkable discoveries in Chinese archaeology in the 20th, the Sanxingdui site (4.4–2.9 ka B.P.) in the Chengdu plain (Fig. 1) of southwestern China confirms the existence of the "disappeared" ancient Shu Kingdom. The unearthed remarkable relics in the eight burial pits of the site, including exquisite large golden masks and a 2.62-m-tall bronze statue of a towering man (Fig. 1a and b), reflected it had a glorious bronze civilization, and advanced the civilization history of the Sichuan region by more than 2000 years [1, 2]. However, there are still many mysteries about this mysterious ancient Shu Kingdom, and among them is the sacrificial culture of the ancient Shu people [3]. The excavation of

*Correspondence:
Fang Xiang
xiangf@cdut.edu.cn
[1] College of Earth Sciences, Chengdu University of Technology, Chengdu 610059, Sichuan, China
[2] State Key Laboratory of Oil and Gas Reservoir Geology and Exploitation, Chengdu University of Technology, Chengdu 610059, Sichuan, China
[3] Institute of Sedimentary Geology, Chengdu University of Technology, Chengdu 610059, Sichuan, China
[4] Sichuan Province Institute of Cultural Relics and Archaeology, Chengdu 610041, Sichuan, China

Fig. 1 Photos of the exquisite cultural relics and geographical background of the Sanxingdui site. **a** Gold mask unearthed from K3 [14]. **b** The 2.62-m-tall bronze statue of a towering man unearthed from K2 [14]. **c** Geographical locations of the cultural regions and the sites mentioned in this paper [34]: (1) Yinxu; (2) Xiaoshuangqiao; (3) Wadian; (4) Erlitou; (5) Sanxingdui; (6) Jinsha; (7) Baodun. The yellow dotted line is the "North Route" of cultural exchange and trade between the ancient Shu Kingdom and China's Central Plain [35]. **d**: Location of the Sanxingdui site

the pits provided a large amount of archaeological data and evidence to research the sacrificial behaviors of the ancient Shu people and explore the evolution of the ancient Shu culture (Fig. 1c), even Chinese culture [4].

The recorded sacrificial rituals in China can be traced back to the Paleolithic Age [5]. During the Shang and Zhou dynasties, various methods such as burning, burying and sinking sacrifices were developed. In some sacrificial rituals, two or more types of methods were combined [5–7].

Burning sacrifice took place all over the world [8–10], the purpose of which was to burn sacrifices to worship ancestors and divinities by using firewood as fuel [11]. The Bible and the Epic of Gilgamesh detailed that the Israelites and Babylonians burned all or only the fat of the divided animal carcasses on the altar to worship their gods [12, 13]. The indigenous people on New Ireland Island (Latangai, Papua New Guinea) still maintain the custom of smashing and burning exquisite wooden carvings to commemorate the deceased [14]. From the

Shang to Qing Dynasties, burning sacrifice was always used by Chinese emperors and nobles in their sacrificial rituals [5]. Nowadays, burning sacrifice is still used by some minorities in China [14, 15]. This kind of sacrificial rituals, burning the offerings after breaking up them, was similar to the sacrificial practices of the ancient Shu people in the Sanxingdui site with some melted and deformed fragments of artifacts buried in the pits after being crushed before burned [16]. However, a large number of the exquisite bronze and jade artifacts used by the ancient Shu people in their sacrifices indicate that the sacrificial behaviors of Sanxingdui have unique ancient Shu culture and religious characteristics, which are different from other parts of the world.

However, archaeologists speculated that the ancient Shu people held burning sacrificial rituals based on historical records and the presence of ash layers and fire-burned artifacts in the burial pits of the Sanxingdui site [17, 18], but they cannot confirm whether the burning sacrificial rituals occurred in the burial pits and whether the pits were used for sacrificial rituals or just used as trash pits to hastily bury damaged sacrificial artifacts caused by wars or other causes [8, 17–25]. Although ancient people's activities of using fire can be speculated through evidence obtained from historical records and the macroscopic characteristics of burnt remains [23, 26], the evidence should be verified by more scientific methods [27]. Chroma and magnetic properties provide objective indicators for exploring the ancients' use and control of fire [28–30]. Because combustion can increase magnetic susceptibility (χ) and chroma redness (a^*) values in sediments [31], researchers have delineated the location of the fire zone at Site No.1 of the Zhoukoudian site in China (Fig. 1c) [32] and estimated the firing temperature of artificial fired materials from Neolithic houses in Bulgaria [33]. Therefore, searching for records related to sacrificial activities in the accumulated materials of the burial pits will provide an important reference for determining the nature of the pits, interpreting such questions about the religious consciousness and behavior patterns of the ancient Shu people [20], whether there was a natural disaster, a change in the monarchy or a war [20–22, 24, 25].

For the above reason, in this article, we comprehensively analyze the geographical location of the pits and the accumulation characteristics of ash layers and artifacts in the pits, measured the chroma and magnetic properties of the soils near the ash layer in representative burial pits 4 and 7 (K4 and K7), and compared them with those of burnt soil debris in the ash layer in K4 and naturally deposit soil near K4. These research results can help us to clarify the purpose of the pits, understand the sacrificial activities of the ancient Shu people in the late Shang Dynasty, and explore the relationship between the Sanxingdui civilization and the Central Plains civilization (Fig. 1c).

Geographical and archaeological background of the Sanxingdui burial pits

The Sanxingdui site (104° 11′ 24″–104° 13′ 12″ E, 30° 59′ 38″–31° 06′ 33″ N) is located in the western suburbs of Guanghan in the northeastern Chengdu Plain (Fig. 1d), with a total area of 12 km^2, and was first excavated in 1929 [14]. According to ancient books and archaeological evidence, it was the capital city of the ancient Shu Kingdom in the Shang Dynasty (c. 3.6–3.0 ka B.P.) [14, 36]. The site is on the southern bank of the Yazi River, which is a branch of the Jian River (a tributary of the Tuo River), and the Mamu River, another branch of the Jian River runs through the site from west to east. Floods and human activities have destroyed many of the rammed earth city walls (Fig. 2a).

The eight burial pits excavated so far (K1–K8) are located in the high-platform terrain area southwest of the site (Fig. 2). The area belongs to the second terrace on the southern bank of the Mamu River [18, 37]. The upper part of the terrace sediments, with a thickness of about 3–4 m, consists mainly of brownish-yellow sandy silt, defined as Guanghan Clay deposited in the late Pleistocene [38–40]. The silt content of the Guanghan Clay increases gradually as the depth increases. The lower part of the terrace sediments gradually transitions to sandy gravel with increasing depth.

Except for the K5 and K6, which are products of the early Zhou Dynasty (ca. 3.0–2.8 ka) shown by unearthed cultural relics, all the pits' depths were between 1.3 m and 2.0 m [18]. Two soil cores were taken from a location roughly 4 m west of the western wall of K4 (K4KP), and almost 5 m east of the eastern wall of K8 (K8E). These two soil cores were obtained from the same elevations as the mouths of K4 and K8, respectively (Fig. 2b). The cores indicate that the soil surrounding the pits can be roughly divided into three layers, from top to bottom (Fig. 3):

(1) 0–20 cm: Natural sediment, brownish-yellow fine-grained sandy silt and silt, containing a few pieces of pottery shards;

(See figure on next page.)

Fig. 2 Location of the study area and related archaeological information [18, 44]. **a** Location of the study area. **b** Planar distribution of burial pits and soil cores. N, E, W, and S refer to the northern, eastern, western, and southern walls of K4 and K8 respectively

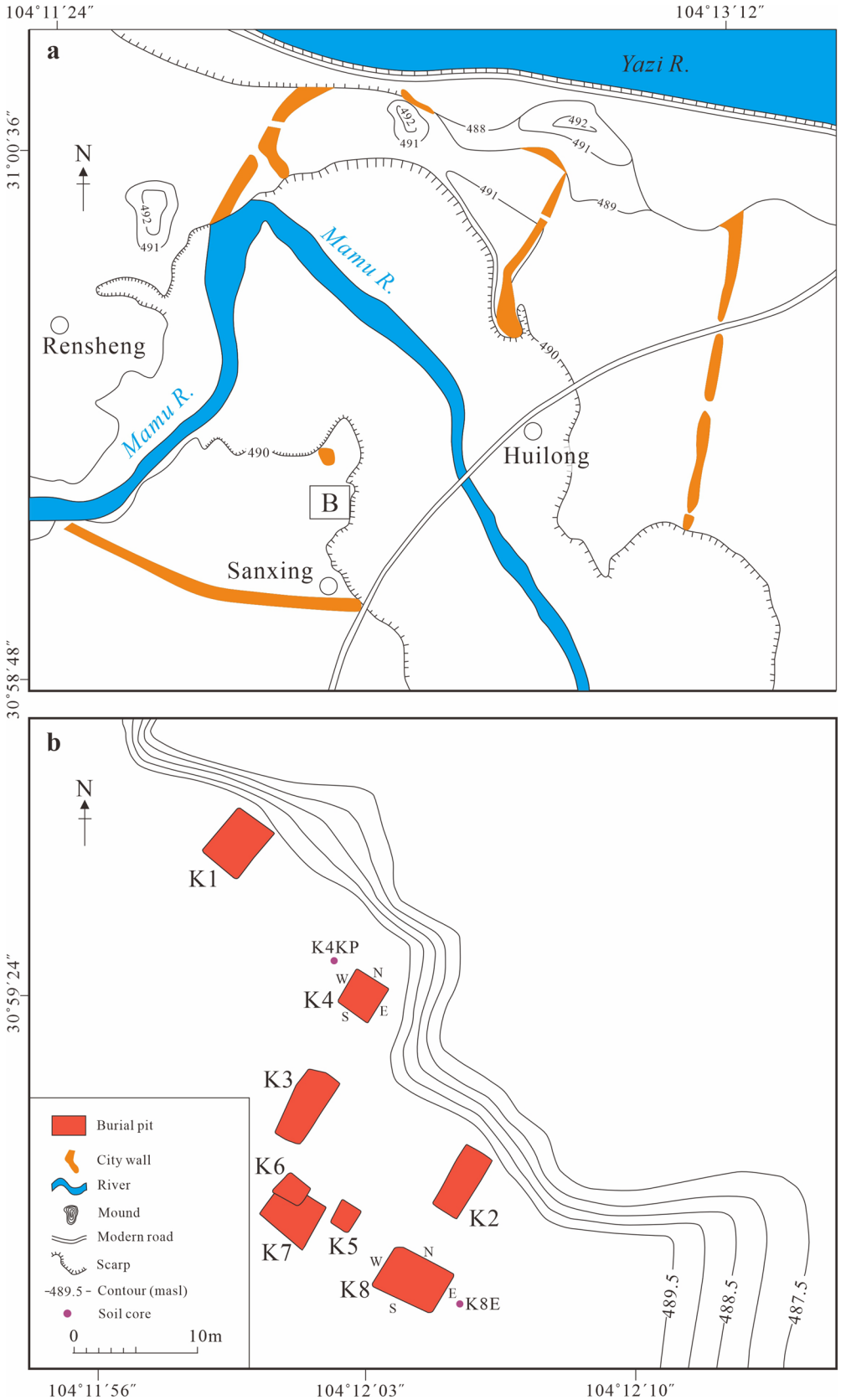

Fig. 2 (See legend on previous page.)

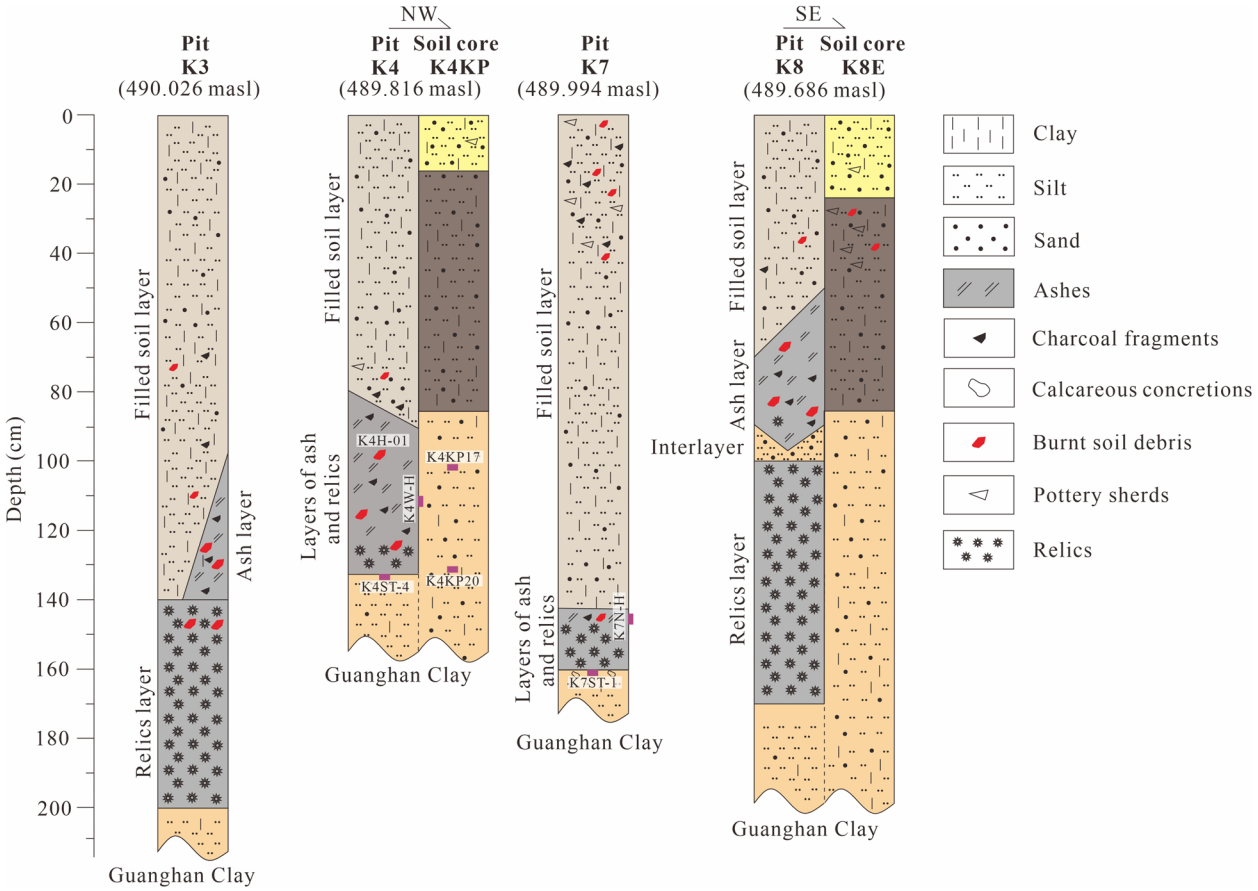

Fig. 3 Characteristics of Sanxingdui burial pits' accumulated materials in pits 3, 4, 7 and 8 (K3, K4, K7 and K8), and of naturally deposit soil near K4(K4KP) and K8 (K8E), and sampling locations

(2) 20–85 cm, brown fine-grained sandy silt with high humus content. Pottery shards and burnt soil debris can be seen in the upper 20 cm thick part of this layer due to disturbance by the ancient Shu people, and the lower part is undisturbed natural sediment;

(3) 85–200 cm, naturally deposited brownish-yellow sandy silt and silt with visible iron-manganese cutans, is Guanghan Clay.

Shapes of artifacts and ^{14}C dating results of ashes indicate that the six pits (K1–K4, K7, K8) are products of the late Shang Dynasty [41, 42]. The remnants of an artifact were scattered in the six pits, further confirming that they were produced simultaneously [43].

The morphology and accumulation characteristics of the six pits are relatively consistent, and different from K5 and K6 (both were only filled by layers of filled soil and relics from top to bottom). All six pits (K1–K4, K7, K8) are composed mainly of layers of filled soil, ashes, and relics from top to bottom, while there is an interlayer consisting of silt with a thickness of 10 to 30 cm between the layers of ash and relics in K8, which is slightly different from other five pits [18]. The filled soil layers are comprised of brown sandy silt and silt, containing pottery pieces, charcoal fragments, and burnt soil debris. The ash layers are uneven and are mainly composed of ashes and charcoal fragments from burnt gramineous plants such as bamboo, reed, rice, and millet [18]. They have no obvious boundaries with the lower relic layers (Fig. 3). Relics, including jade wares, pottery, and gold wares, dominate the bottoms of the pits [17]. The main jade wares are relatively intact, while the minor ones are fragments broken in situ. The pieces of pottery and gold wares are scattered at the bottoms of the pits, and bronze wares and fragments cover them. The large bronze wares are at the upper layers, and the small wares and fragments of bronze are at the lower layers. The bronze pieces were mainly the result of in situ crushing, and the rest formed from crushing outside the pits. Above them are the ivories scattered all over the pits. The ancient Shu people burned all the relics to varying degrees in burning sacrificial rituals [14]. The six burial pits (K1–K4, K7, K8) formed simultaneously at the Sanxingdui site all have

regularly overlaying characteristics, and the relics in the pits have been burned to varying degrees, reflecting that they all likely have been used for the same purpose. All the ash layers of the pits have inclined dumping characteristics. Although ash layers are found in a single corner of K2 and K3, while an interlayer is present between the ash layer and the burnt relics layer in K8 [18]. These evidences indicate that the relics scattered all over these three pits were not burnt in the pits. However, because the ashes and charcoals scattered all over the lower parts of K1, K4 and K7, and in contact with the pits' walls, bottoms and burnt relics layers, it is difficult to determine whether the burning sacrificial rituals occurred in the three pits only depending on the archaeological evidence. Therefore, K4 became the ideal object for our research due to its ash layer was thickest (Fig. 3) and K1 was backfilled after rescue excavation in the 1980s. In addition, we also analyzed K7 as supplements to demonstrate the reliability of the results.

Sedimentary characteristics and sampling collection of soils in and near K4 and K7

K4 is located on the north side of the excavation area of the burial pits, its mouth is approximately square (about 8.3 m^2), and the elevation is 489.816 m (Figs. 2, 3). The depth of K4 is about 1.4 m (Fig. 3), and the four walls of K4 are vertical and flat. The soils near the ash layer of K4, brownish yellow sandy silt and silt, are consistent with Guanghan Clay (Fig. 3). The upper surface of K4's ash layer inclines from the southeastern corner to the northwestern corner, the thickness of the ash layer in contact with the western wall of K4 is about 0.4 m (Fig. 3). Its components are charcoal fragments, ashes, and a small amount of irregular burnt soil debris (Fig. 3). The burning of clayey silt and silt formed the burnt soil debris. Although the surfaces of the burnt soil debris are dark red due to carbonaceous contamination during long-term buried after burnt, it has retained the morphology and grain-size characteristics of Guanghan

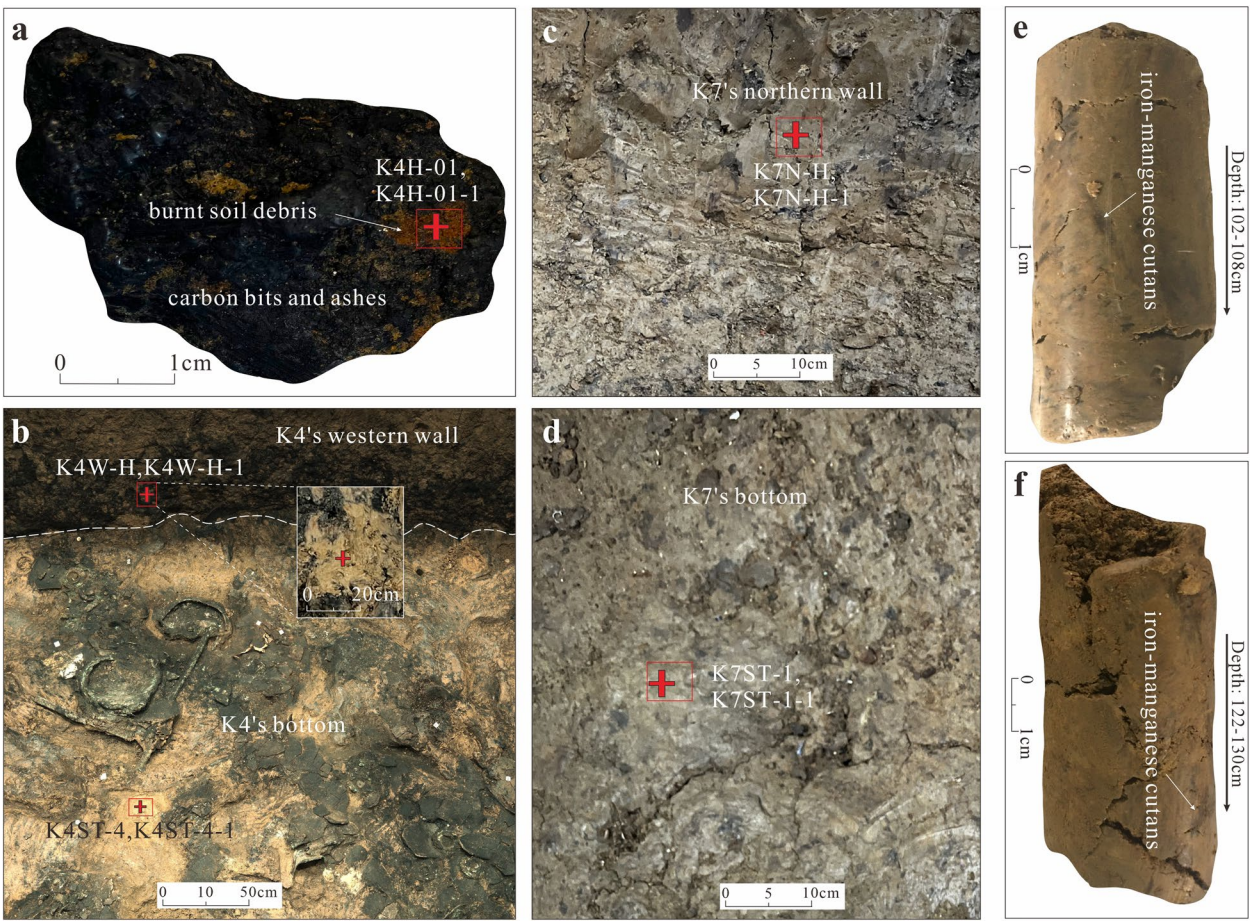

Fig. 4 Characteristics of burnt soil debris, soils and Guanghan Clay. **a** Sampling and in-situ test locations at the burnt soil debris in K4's ash layer. **b** Sampling and in-situ test locations at the western wall and bottom of K4. **c** Sampling and in-situ testing locations at the western wall of K7. **d** Sampling and in-situ testing locations at the bottom of K7. **e**, **f** Iron-manganese cutans can be seen in Guanghan Clay in core K4KP (K4KP17, K4KP20). The depth gradually increases along the arrow direction. The red cross symbols are the in-situ testing points of magnetic susceptibilities

Clay (Fig. 4). The filled soil layer in K4 covering the ash layer with an average thickness of about 85 cm (Fig. 3). The buried deep filled soil mixed pottery pieces, charcoal fragments, and burnt soil debris (Fig. 3).

Although compared with K4, K7 is deeper and has a thinner ash layer, the morphology and accumulation characteristics of the two pits are similar. The soils near the ash layer in K7 are comprised of brownish-yellow sandy silt and silt, and are consistent with Guanghan Clay [40].

After clearing the surface charcoal fragments and ashes, we used a portable magnetic susceptibility meter to in-situ test the magnetic susceptibilities of the burnt soil debris (K4H01-1) in K4's ash layer and the soils near the ash layers of K4 and K7 near the ash layers (K4W-H-1, K4ST-4-1, K7NW-H-1 and K7ST-1-1). Furthermore, samples were collected from the positions of in-situ testing in K4, including burnt soil debris (K4H-01) in K4's ash layer and the soils near the ash layer (K4W-H and K4ST-4), for laboratory magnetic property analysis. In addition, chroma samples were collected from K4 at the same positions as the in-situ magnetic susceptibilities test and from K7, including the soils near the ash layer of K7 (K7NW-H and K7ST-1). Meanwhile, samples of Guanghan Clay with depths of 105 cm and 130 cm (K4KP17 and K4KP20) were collected from K4KP for chroma and magnetic property analysis (Figs. 2, 3, 4, Table 1).

Methods

Identifying clear evidence of humanly-controlled fire in K4 and K7 is a challenging task because the ashes and charcoals were scattered all over the lower parts of the pits and in contact with the pits' walls, bottoms, and burnt relics layers. The characteristics of grain sizes, contents, and types of iron minerals in sediments, such as magnetite and hematite, can easily change due to the impact of human use of fire. Therefore, data of chroma and magnetic properties are used to determine whether sediments in archaeological sites were affected by the fire used by the ancients. Chroma data can be accurately measured by spectrophotometer while magnetic properties can be measured by portable magnetic susceptibility meters and laboratory magnetic property analyses. Portable magnetic susceptibility meters have the advantage of simple operation, convenient use, and high sensitivity for in situ measurements. So, we used a portable magnetic susceptibility meter to measure the burnt soil debris in ash layer of K4 and soils near the ash layer of K4 and K7. However, the accuracy of the meter's results may be influenced by environmental magnetic fields. To demonstrate the reliability of the results, we sent the samples in K4 which tested by the meter to laboratory to measure magnetic properties. Finally, we discuss whether the ancient Shu people held burning sacrificial rituals in burial pits by integrating the data of chroma and magnetic properties.

In-situ test of magnetic susceptibilities

After the surface charcoal fragments and ashes at the test points had been cleared, a KT-10 field portable magnetic susceptibility meter (TERRAPLUS and GEORADIS s.r.o., Error is 1×10^{-6} SI, operating frequency 10 k Hz) used for in-situ measure the magnetic susceptibility (κ) of the burnt soil debris in ash layer of K4 and soils near the ash layer of K4 and K7. The value of κ reflects the total magnetic mineral concentration of sediments, dominated by ferrimagnetic minerals (e.g., magnetite, maghemite) and anti-ferromagnetic minerals (e.g., hematite, goethite).

When testing, position the instrument probe tightly against the burnt soil debris or fresh surface of the soil

Table 1 Summary of sampling and in-situ testing point information in the Sanxingdui site

Numbers of in-situ testing and sampling	Samples attribute and sampling or testing location	Sediment characteristics
K4ST-4 (lab) K4ST-4-1 (in-situ test)	A representative soil sample from K4's bottom (depth = 134 cm) in contact with the ash layer	Brownish-yellow sandy silt and silt
K4W-H (lab) K4W-H-1 (in-situ test)	A representative soil sample from K4's western wall (depth = 110 cm) in contact with the ash layer	
K4H-01 (lab) K4H-01-1 (in-situ test)	Representative burnt soil debris in K4's ash layer (depth of about 100 cm)	Irregular clayey silt and silt soil debris with dark red
K7N-H (lab) K7N-H-1 (in-situ test)	A representative soil sample from K7's northern wall (depth = 142 cm) in contact with the ash layer	Brownish-yellow sandy silt and silt
K7ST-1 (lab) K7ST-1-1 (in-situ test)	A representative soil sample from K7's bottom (depth = 161 cm) in contact with the ash layer	
K4KP17 (lab)	Guanghan Clay with a depth of 105 cm, about 4 m to the western side of K4's western wall	Brownish-yellow sandy silt and silt, visible iron-manganese cutans
K4KP20 (lab)	At the same location as K4KP17, and the depth is 126 cm	

(avoiding cracks, pottery sherds, and burnt soil debris) after resetting the instrument, and keep the pickup coil of the instrument parallel to the fresh surface. At the same time, press the measurement button again, and the instrument display screen will show the magnetic susceptibilities of the soil. Repeat the above operation at least three times for each test point and record the results. Finally, calculate the average magnetic susceptibilities of the soil, respectively.

Laboratory measurement of chroma and magnetic properties

To reduce experimental error, we naturally dried soil samples at room temperature before sending them to the laboratory for chroma and magnetic properties tests.

Chroma measurement

Chroma measurement is an effective method for exploring the composition and content of magnetic minerals in sediments [48]. The measurements were completed at Chengdu University of Technology, using the KONICA MINOLTA CM-700d spectrophotometer (light source 10°/D65, standard deviation of chroma values $\Delta E^*_{ab} < 0.04$). The CIELAB system, which consists of brightness (L^*), redness (a^*), and yellowness (b^*), is used to describe the chroma of samples quantitatively [49]. The naturally exposed surfaces of the samples were trimmed to a flat surface with a moderate size before measurement, keeping the calibrated instrument measuring port close to the surface, and iron-manganese cutans of the samples should be avoided during the test. Read three sets of results for each sample and take mean values: ΔL^*, Δa^*, and Δb^*.

Carbonaceous contamination will reduce the chroma values of the sample [50–52]. However, the contamination does not affect the ratio of the chroma values of two different wavelengths obtained from the same position of a sample surface [53–55]. Therefore, in this study, the ratio of $\Delta a^*/\Delta b^*$ is used to investigate the composition and relative content of magnetic minerals in the samples.

Magnetic properties measurement

Magnetic properties can effectively reflect changes in the composition, concentration and grain size of magnetic minerals in sediments caused by combustion [56, 57]. Magnetic properties were measured at South China Normal University. Fine-grained samples were packed into non-magnetic cubic boxes ($V = 8$ cm^3) and weighed.

Values of mass susceptibilities (χ), including low- and high-frequency mass susceptibilities (χ_{lf} and χ_{hf}), were obtained as volume low- and high-frequency magnetic susceptibilities (κ_{lf} and κ_{lf}) divided with the sample density. κ_{lf} and κ_{lf} measured by Kappabridge MFK1-FA (AGICO, error < ± 0.1%) at low (976 Hz) and high frequency (15,616 Hz) and under low fields (200 m/A). As used here, κ refers to κ_{lf}, and χ refers to χ_{lf}. The value of χ indicates the total magnetic mineral concentration of sediments. Compared to multi-domain (MD) particles, single-domain (SD) particles can obtain strong susceptibility of anhysteretic remanent magnetization (χ_{ARM}) [58], so χ_{ARM} is often used to measure the content of single domain particles in sediments [59, 60]. χ_{ARM} was the result of the anhysteretic remanent magnetization (ARM) divided by the direct current (DC) bias (0.05 mT), the ARM was measured by a JR-6A Spinner Magnetometer (AGICO, error < 1%). The value of saturation isothermal remanent magnetization (SIRM) positively correlates with the total concentration of magnetic minerals primarily and magnetic crystal grain size secondarily, but irrelevant with superparamagnetic (SP) domains. We used an IM-10-30 Impulse Magnetizer to impart SIRM to the Z-axis for each sample at a DC field of 1T and was measured by the JR-6A Spinner Magnetometer. Both frequency-dependent magnetic susceptibility (χ_{fd}) and percentage frequency-dependent magnetic susceptibility (χ_{fd}%) values reflect the relative content of SP/SD boundary of magnetic minerals in sediments [61, 63]. The higher the values, the finer the magnetic minerals are [58–60]. χ_{fd}% was calculated from $\chi_{fd}\% = [(\chi_{lf}\text{-}\chi_{hf})/\chi_{lf}] \times 100\%$. Different χ_{fd}% values indicate different proportions of SP magnetic minerals in sediments: $\chi_{fd}\% < 5\%$, SP magnetic minerals do not dominate the magnetic mineral assemblage; $\chi_{fd}\% > 5\%$, contained a high proportion of SP magnetic minerals [61]. Isothermal remanent magnetizations (IRM_{-300mT}) of the samples were measured under the back-field (-300 mT), and values of "hard" isothermal remanent magnetization (HIRM) were computed using the formula $HIRM = (SIRM + IRM_{-300mT})/2$ [62]. The high value of HIRM reflects the high absolute content of high coercive minerals such as hematite or goethite in the soil. In addition, S_{-300} was calculated using the formula $S_{-300} = (SIRM\text{-}IRM_{-300mT})/(2 \times SIRM)$ [62]. S_{-300} close to 1 indicates a high proportion of low coercively minerals such as magnetite and maghemite, while a low ratio (close to 0) indicates a high proportion of high coercively [59–61].

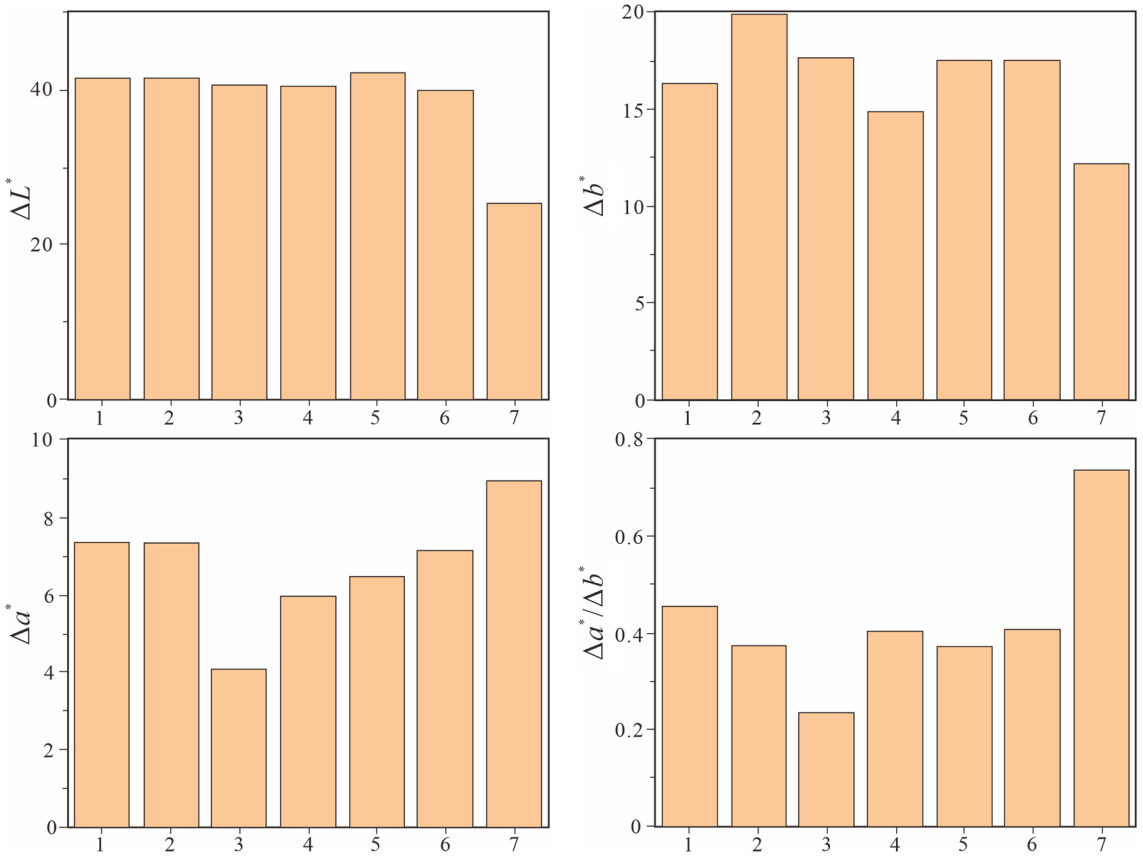

Fig. 5 Chroma characteristics of burnt soil debris, soils and Guanghan Clay. The numbers on the horizontal axis represent the sample code: (1) K4W-H; (2) K4ST-4; (3) K7N-H; (4) K7ST-1; (5) K4KP17; (6) K4KP20; (7) K4H-01

Results

Chroma

The chroma values and $\Delta a^*/\Delta b^*$ ratios of soils near the ash layers of K4 and K7 are similar to those of Guanghan Clay near K4 (Fig. 5).

Although the values of ΔL^* and Δb^* of burnt soil debris in K4's ash layer are lower than that of other samples due to the influence of carbonaceous contamination, the value of Δa^* of the debris is higher than other samples because of the base value of it is high (Fig. 5).

Consequently, the $\Delta a^*/\Delta b^*$ ratio of burnt soil debris is 0.74, which is significantly higher than other samples (Fig. 5).

Magnetic properties

The κ values of soil near the ash layer of K4 and the burnt soil in the ash layer, measured by KT-10, are consistent with the data obtained in the laboratory (Fig. 6), indicating that the results of KT-10 are reliable and can be compared with laboratory results. The κ values of soils near the ash layers of K4 and K7 are similar to that of Guanghan Clay near K4, significantly lower than that of the burnt soil debris (Fig. 6).

The values of χ, χ_{fd}, χ_{ARM}, SIRM, and HIRM in the soils near the ash layer of K4 are similar to those of Guanghan Clay near K4, but significantly lower than those of burnt soil debris in K4's ash layer (Fig. 6). χ_{fd}% of burnt soil debris is above 6%, while the values of the soils near the ash layer of K4 and Guanghan Clay near K4 are below 6% (Fig. 6).

(See figure on next page.)

Fig. 6 Magnetic properties characteristics of burnt soil debris, soils and Guanghan Clay. The numbers on the horizontal axis represent the sample code: (1) K4W-H; (2) K4W-H-1; (3) K4ST-4; (4) K4ST-4-1; (5) K7N-H-1; (6) K7ST-1-1; (7) K4KP17; (8) K4KP20); (9) K4H-01; (10) K4H-01-1

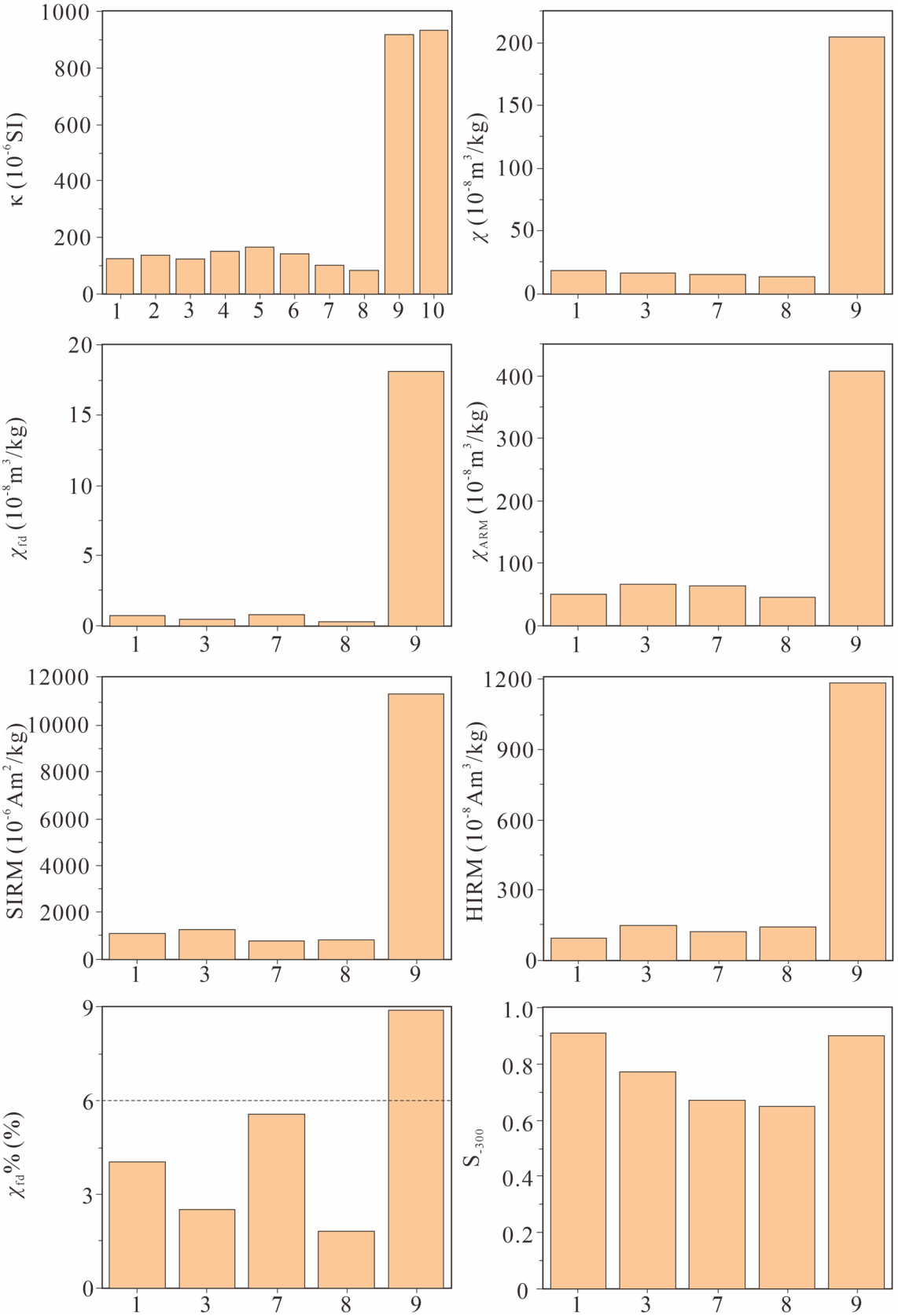

Fig. 6 (See legend on previous page.)

The S_{-300} value of burnt soil debris is approximately 0.90, close to the value of the soil from K4's western wall, higher than the values of the soil from K4's bottom (0.77) and Guanghan Clay near K4 (0.66) (Fig. 6).

Discussion

Indicative significance of chroma characteristics

The combustion temperature is generally closely related to the species of plants used as fuel [63, 64]. The ashes in the burial pits were mainly formed by burnt gramineous plants (such as bamboo, reed, rice and millet) growing in the Chengdu Plain in the Shang Dynasty [18, 65]. The ignition point of gramineous plants is about 300 ℃ and they are completely carbonized and gradually incinerated when the temperature reaches 400 ℃ [64, 66, 67]. In addition, serpentine jade and tremolite jade are gradually bleached after dehydration and iron oxidation reactions at 500–600 ℃ [68, 69].

The ashes in the pits are composed of carbonized and incinerated gramineous plants, and some serpentine jade and tremolite jade unearthed from the pits show partial bleaching caused by burning sacrificial rituals [70, 71], indicating the temperature of the rituals could be reached or above 500–600 ℃. Furthermore, the highest burning temperature of the open-air fire used by the ancient Shu people in the late Shang Dynasty was about 800 ℃ [72]. Consequently, we consider that the temperature of the ancient Shu people burning sacrifices could be 600–800 ℃ in the late Shang Dynasty, which is consistent with the views that the temperature of the ancients' use of fire could be above 600 ℃ [30, 73].

Previous research suggested that lepidocrocite (γ-FeO(OH)) transforms to maghemite (γ-Fe_2O_3) at 300 ℃ and this may further transform to hematite at 350 ℃ [74–76]. In addition, goethite (α-FeO(OH)) converts to hematite (α-Fe_2O_3) through the dehydration process when the combustion temperature exceeds 400 ℃ [77–80]. Hematite is a typical dye mineral that can redden soil significantly [78, 81]. The value of $\Delta a^*/\Delta b^*$ can effectively reflect the ratio of hematite to goethite in soil [81–85].

The calculation results show that the ratios of $\Delta a^*/\Delta b^*$ of soils near the ash layers of K4 and K7 are close to that of Guanghan Clay near K4, but significantly lower than that of burnt soil debris in K4's ash layer (Fig. 5). It indicates that the temperature of the burning sacrificial rituals can prompt a significant part of the goethite in the soil to transform into hematite, reflecting the burning temperature above 400 ℃. However, the soils near the ash layers of K4 and K7 do not appear to have been heated sufficiently to change their chroma, indicating that burning sacrificial rituals do not occur in the pits.

Indicative significance of magnetic properties

The high temperature and reductive gas environment generated in the fire process used by the ancients promoted the iron-containing silicate minerals and clay minerals in the soil to transform into fine ferromagnetic minerals, including SP and SD magnetite [46, 86]. This environment also promoted the conversion of some anti-ferromagnetic minerals in the soil into ferromagnetic minerals [46, 86]. In addition, the hematite formed by the dehydration of goethite in the soil through the fire used by the ancients is generally SP grain size [79]. The transformation of these magnetic minerals can significantly increase the values of the magnetic susceptibility of soil [31, 51, 56, 57, 87]. The κ and χ values of soils near the ash layers of K4 and K7 are similar to those of Guanghan Clay near the pits. The values are 1/5–1/11 (κ) and 1/11–1/15 (χ) of that of burnt soil debris in K4's ash layer (Fig. 6), indicating that K4 and K7 were not affected by human use of fire.

Analysis results show that the burnt soil debris in K4's ash layer has a high content of magnetic minerals (Fig. 6), and almost all minerals are ferromagnetic (Fig. 6). In addition, HIRM values and $\Delta a^*/\Delta b^*$ ratios show that the burnt soil debris in K4's ash layer contains a relatively high content of imperfect anti-ferromagnetic minerals, mainly hematite (Figs. 6, 7). Ferromagnetic minerals and hematite content in soils near the ash layer of K4 are similar to those in Guanghan Clay near K4, but significantly lower than those in the burnt soil debris (Fig. 6).

The results show that soils near the ash layer of K4 contain tiny SD and SP magnetic minerals, and the ratio of SP magnetic minerals to total magnetic minerals in the soil is negligible. It is similar to Guanghna Clay near K4, but contrary to burnt soil debris in the K4's ash layer (Fig. 6). These resulted in the χ values of soils near the ash layer of K4 that were similar to Guanghan Clay but significantly lower than the value of burnt soil debris (Fig. 7).

It is considered that the magnetic mineral compositions and contents of the soils near the ash layers of K4 and K7 are similar due to the macro-sedimentary characteristics, and the values of chroma and magnetic susceptibilities, of the soils are relatively consistent with the Guanghan Clay. Therefore, the contents of fine ferromagnetic minerals and hematite in soils near the ash layers of K4 and K7 are less than that of burnt soil debris but similar to Guanghan Clay, indicating that ancient Shu people did not hold burning sacrificial rituals in the pits.

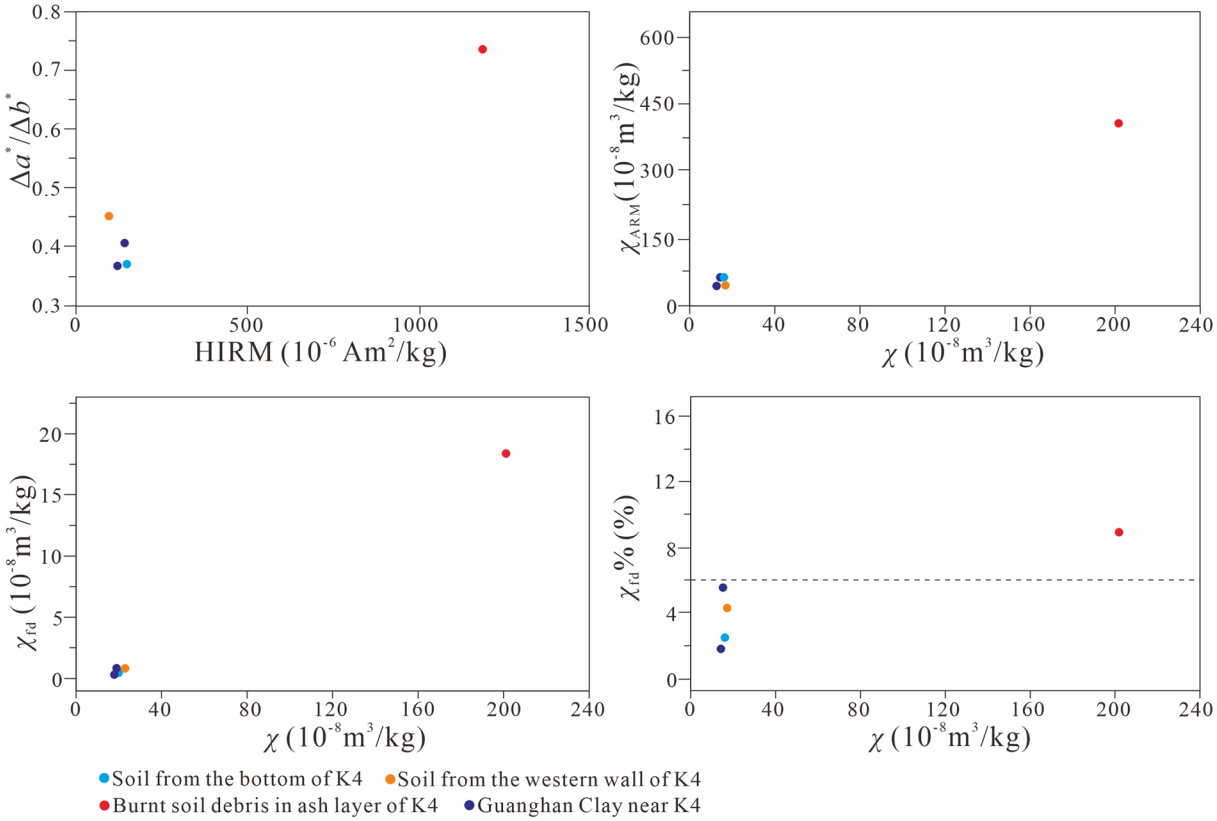

Fig. 7 Biplots of magnetic properties and chroma of burnt soil debris, soils and Guanghan Clay

The relationship between the sacrificial cultures of the ancient Shu Kingdom and China's Central Plain in the late Shang Dynasty

According to the chromaticity and magnetic properties of burnt soil debris in the ash layer of K4, the soils near the ash layers of K4 and K7, and the Guanghan Clay near K4, combined with the accumulation characteristics of ash and relics layers in K2, K3 and K8 [14, 18], we consider that the ashes and burnt relics were buried after the burning sacrificial rituals outside the pits formed in late Shang Dynasty. Archaeological excavations reveal that sacrificial rituals in China's Central Plain during the Shang and Zhou Dynasties were mainly performed in the high platform terrain area [1, 5, 88]. The burial pits formed after burying sacrificial rituals (a kind of sacrificial ritual in which sacrifices are stacked in the pits in order and buried) at the Jinsha site (Fig. 1c) in the early Zhou Dynasty are also concentrated on a high platform [23, 89, 90]. The nature of the Sanxingdui burial pits is currently controversial. Some scholars believed that the pits were used to bury trash artifacts that were damaged by different reasons (such as a change in the monarchy or a war), and these pits did not have any religious purpose or sacrificial significance [15, 20]. The reason is that these burial pits were formed at the same time, but the shapes and quantities of buried artifacts in each pit vary greatly, which is different from the results of the traditional burying sacrificial rituals [43, 91]. However, these pits are concentrated in the high platform terrain area southwest of the site (Fig. 2), the shapes and overlap characteristics of the pits are regular, and they are compacted during the burial process. Moreover, the ancient Shu people buried the ivories, which were sacred sacrificial artifacts and were believed to have the function of communicating with the gods [91], on the bronze and jade artifacts in each pit during the burial process. The evidence reflects that the pits are burial places with uniform sacrificial rules, rather than the result of hasty burial, and the burial activities were devout and orderly rituals. Based on the above analysis, combined with the burial pits were formed before the ancient Shu people migrated from the Sanxingdui site due to the irresistible catastrophic events, such as natural disasters or defeat in a war, which led to the decline of the Sanxingdui civilization [92–94], we consider that the ancient Shu people forced to hold a series of sacrificial rituals to pray for the gods to eliminate the disasters, and the rituals went through two stages successively: (1) burnt sacrifices; (2)

buried the burnt sacrifices underground. The pits were products of burying sacrificial rituals rather than buried trash artifacts [20, 22–24].

Many bronze and jade wares unearthed at the Sanxingdui site and the metallurgical technology of the ancient Shu Kingdom have high similarities with China's Central Plain, such as Yinxu [14, 35] (Fig. 1c), reflecting that there was a close cultural exchange between the ancient Shu Kingdom and China's Central Plain. Archaeologists considered that the exchange was mainly through the "North Route" [35] (Fig. 1c). In addition, the shape of some Gaobingdou (a kind of pottery food container) and other instruments unearthed at the Sanxingdui site are identical to the Erlitou site (Fig. 1c) in Yanshi, Henan Province [95]. It indicates that the cultural exchange between the two regions probably originated as early as the Xia Dynasty (4000–3600 a B.P.) or even the Longshan period (4350–3950 a B.P.) [96–98] (Fig. 8). Although archaeological excavation data from the Wadian site (Fig. 1c) in Yuzhou, Henan Province, reveal that rituals of burying sacrifice after burning sacrifice have already occurred in China's Central Plain during the Longshan period (4.3–4.0 ka) [99], there are no remains of the rituals in the Baodun site (Fig. 1c) during the same period due to the preliminary and incomplete initial stage of cultural exchange [52] (Fig. 8). Subsequently, China's Central Plain culture significantly influenced the ancient Shu culture in the Shang Dynasty (3.6–3.0 ka B.P.) with the deepening of cultural exchange [100]. At that time, the rituals of burying sacrifice after burning sacrifice occurred in China's Central Plain [5, 15, 101]. Archaeological evidence and test data obtained by integrating sphere spectrophotometer, X-ray fluorescence (XRF), scanning electron microscope (SEM), infrared reflectance spectroscopy and Raman spectra indicated that burnt soil debris and sacrifices, which unearthed from the Xiaoshuangqaio site and Yinxu site in China's Central Plain, experienced the rituals of burying sacrifice after burning sacrifice [102–104] (Fig. 1c)Thus, ancient Shu people began to hold the rituals of burying sacrifice after burning sacrifice under the influence of many factors (such as war, change of royal power, climate deterioration, etc.) in the late Shang Dynasty (~3.0 ka B.P.) indicates that China's Central Plain culture probably influenced the sacrificial rituals performed by the ancient Shu people (Fig. 8). However, the sacrifices used in the

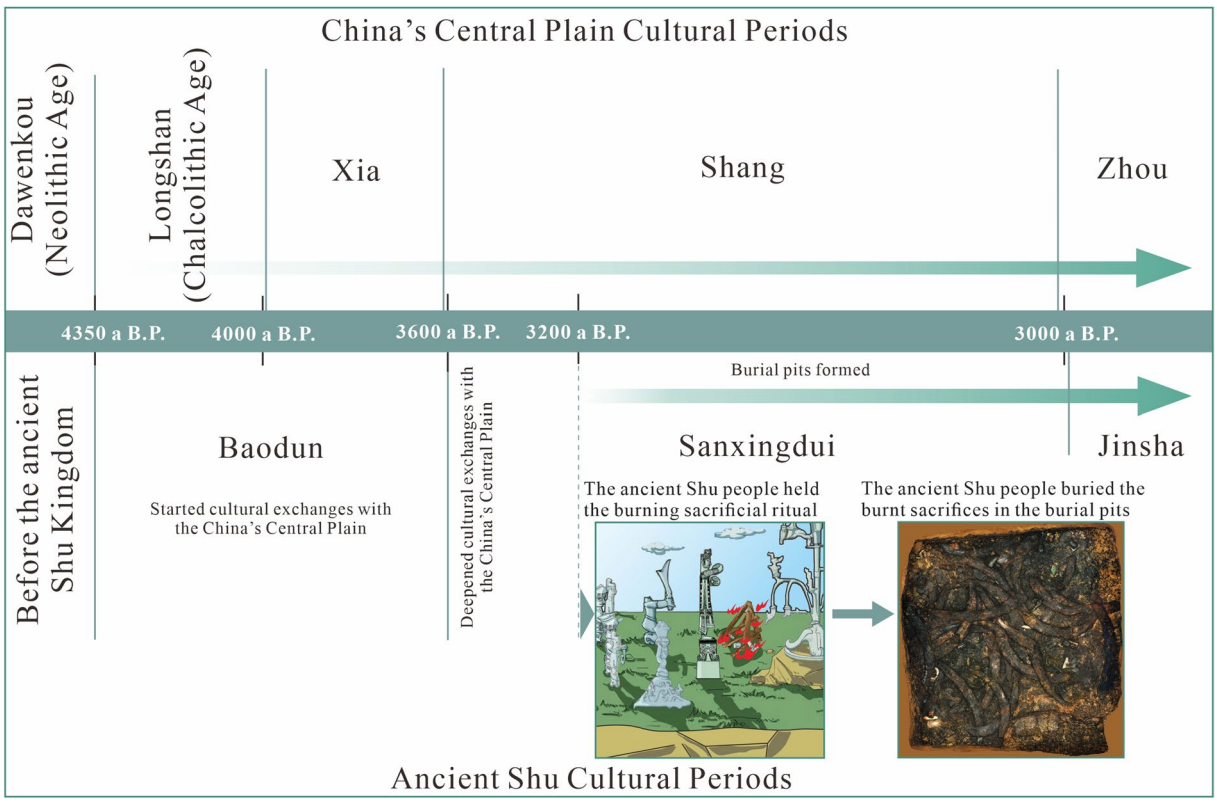

Fig. 8 Compare the appearance time of the burying sacrifice after burning sacrifice between the ancient Shu Kingdom and China's Central Plain. The arrow direction shows the process of the emergence and evolution of sacrifice. The reconstruction picture of the sacrificial scene of the ancient Shu people in the late Shang Dynasty is modified from Tang [16]. The photo of the burial pit at Sanxingdui site is cited from Ran et al. [18]

sacrificial ritual, such as ivory and bronze masks, and the large scale of the burial pits, reflecting a completely different sacrificial culture compared to China's Central Plain during the same time [5, 90, 100, 105].

Conclusion

From the characters of the charcoal fragments, ashes and jades in the Sanxingdui buried pits, combined with the previous research results, we speculated that the temperature of burning sacrificial rituals carried by the ancient Shu people in the late Shang Dynasty could have reached 600–800 ℃. This burning temperature can lead to significant changes in the color and magnetic mineral composition of the soil. However, the $\Delta a^*/\Delta b^*$ ratios and magnetic susceptibilities of the soils near the ash layers of K4 and K7, and the contents of the fine-grained (SP, SD) ferromagnetic minerals and hematite of soils in K4 and K7, are similar to those of Guanghan Clay near K4 and are significantly lower than those of burnt soil debris. Meanwhile, the ash layers in the pits present dumping characteristics, and a silty interlayer appears between the ash and relics layers in K8. These evidences indicate that the burning sacrifice did not be held in the Sanxingdui burial pits. Burial pits are distributed in the high platform terrain area in the southwest of the Sanxingdui site, and the artifacts in the pits have been stacked in a specific order. Those characteristics of burial pits indicate that the sacrificial rituals of ancient Shu people in the late Shang Dynasty included two steps: first burning in some suitable place, then burying in the pits. So, these pits were sacrificial pits and not trash pits.

During the Longshan period (4.3–4.0 ka BP) in China's Central Plain, archaeological sites have revealed the practice of burying sacrifice after burning sacrifice. However, the Sanxingdui sacrificial pits of the Shu Kingdom that emerged in the late Shang Dynasty (~3.0 ka BP) were unique in their large scale and the nature of their sacrifices. This suggests that despite being influenced by the Central Plain culture, the ancient Shu people of the late Shang Dynasty had their own distinct cultural and religious features.

Acknowledgements
The Authors thank the editors and several anonymous reviewers for their constructive comments and suggestions.

Author contributions
YG and FX contributed to the conceptualization, methodology, validation, investigation, data curation, writing main manuscript text and visualization. HR, ZX, QY, HH and LD contributed to the investigation and visualization. All authors read and approved the final manuscript.

Funding
This study was supported by the Sanxingdui Science and Technology Archaeology Project of Chengdu University of Technology (No. 21700-000510) and Project of Research on Burial Characteristics of Sanxingdui Sacrificial Pit 4 (No. AHM061).

Availability of data and materials
The datasets used and/or analyzed during the current study are available from the corresponding author on reasonable request.

Declarations

Ethics approval and consent to participate
Not applicable.

Consent for publication
All authors approved the final manuscript and the submission to this journal.

Competing interests
The authors declare no competing interests.

Received: 13 September 2023 Accepted: 29 November 2023
Published online: 06 December 2023

References

1. Sun H. Bronze age in Sichuan Basin. Beijing: Science Press; 2000. (**in Chinese**).
2. Tian H, Zeng XT, Guo JB, Qu L, Chen KL. X-ray computed tomography reveals special casting techniques used with unusual bronze objects unearthed from the Sanxingdui site. Adv Archaeomater. 2022;3:28–33.
3. Ran HL. A preliminary study on the sacrificial remains in the Ancient Shu Region. Sichuan Cult Relics. 2022;6:80–97 (**in Chinese**).
4. Yang B. Enriching ancient history with archaeology: enlightenment and mystery of sanxingdui Site. Chinese Cult Res. 2022;2:73–9.
5. Zhang YY. The research for sacrifice remains in Xia, Shang, and Zhou Dynasties. Shaanxi: Northwestern University; 2019. (**in Chinese**).
6. Jing ZW. A preliminary study on the Prehistoric sacrificial remains. Northern Cult Relics. 2002;2:6–15 (**in Chinese**).
7. Wang R, Tian YQ. The archaeological evidence of the Liao Sacrifice (burnt offering) of jade objects at the Xuechi Site in Fengxiang. Archaeol Cult Relics. 2020;6:98–103 (**in Chinese**).
8. Chen XD, Chen DA. An analysis of the attribution and related problems of the No. 1 Pit in the Shang Dynasty at the Sanxingdui Site. Cultural Relics. 1987;4:4 (**in Chinese**).
9. Chinchilla O. Fire and sacrifice in Mesoamerican myths and rituals. In: Andrew S, Vera T, editors. Smoke, flames, and the human body in Mesoamerican ritual practice. Washington: Dumbarton Oaks; 2018. p. 29–53.
10. Fu YG, Liang YJ, Liu Y, Kister DA. Blood sacrifice and fire rituals. In: Fu YG, editor. Shamanic and mythic cultures of ethnic peoples in Northern China I. London. New York: Routledge Press; 2020.
11. Xu JX. Burnt sacrifice, imperial mountain-top worship of Heaven and Earth, and hall circlet Architecture. Chinese Characters. 1967;5:19 (**in Chinese**).
12. Eberhart CA. A Neglected feature of sacrifice in the Hebrew Bible: remarks on the burning ritual on the Altar. Harvard Theol Rev. 2004;97:485–93.
13. Nie WQ. Discovery and study of the sacrificial remains of Songze and Liangzhu Cultures in the area around the Taihu Lake. Nanjing: Nanjing Norm. Univ; 2019. (**in Chinese**).
14. Zhao WJ. New archaeological marvels of ancient Shu civilization. Natl Sci Rev. 2021;7: nwab071.
15. Xu K. Things used in Liao Sacrifice in Ancient China and its significance. J Sichuan Univ. 2008;3:138–43 (**in Chinese**).
16. Tang JG. "Sacrificial Pits" or "National annihilation Pits": a game of viewpoints behind archaeology of Sanxingdui. Orientations. 2021;3:6–25 (**in Chinese**).
17. Chen XD. Study on bronzes of the Sanxingdui Site. Guanghan Sichuan Cult Relics. 1990;6:22–30 (**in Chinese**).
18. Ran HL, Lei Y, Zhao H, Xie ZB, Li HC, Wang C, et al. Sacrificial area of the Sanxingdui Site in Guanghan City, Sichuan. Archaeology. 2022;7:15–33 (**in Chinese**).

19. Chen XD. Discussion on two problems of Pit 1 and 2 in the Sanxingdui Site, Guanghan. Cult Relics. 1989;5:36–8 (**in Chinese**).
20. Lin X. The origin of Sichuan wine: a study in the Shaman culture in ancient Sichuan. Southern Ethnol Archaeol. 1987;1:73–84 (**in Chinese**).
21. Xu CL. Different views of "Buried Pit Theory" of Sanxingdui-also discussion on the relationship between Yufu and Duyu periods. Sichuan Cult Relics. 1992;5:32–8 (**in Chinese**).
22. Sun H. Analysis of the age and attribution of Sanxingdui artifact pits. Cult Relics. 1993;11:71–6 (**in Chinese**).
23. Zhao DZ. Discuss on the sacrifice form of Sanxingdui. Sichuan Cult Relics. 2018;2:59–73 (**in Chinese**).
24. Sun H. The burial of sacrificial pits in Sanxingdui: burial nature, archaeological dating, pits owner and background. Southern Ethnol Archaeol. 2013;9:9–53 (**in Chinese**).
25. Shi JS. Reviewing of Sanxingdui artifact pit. Acta Archaeologica Sinica. 2004;2:157–82 (**in Chinese**).
26. Ozán IL, Orgeira MJ, Buscaglia S, Villelli MB, V'asquez CA, Cieplicki A, et al. Sediments vs. Historical narratives: the use of soil magnetic properties to evaluate the existence of a historical fire in an 18th century Spanish fort (Patagonia, Argentina). J Archaeol Sci Rep. 2020;34: 102577.
27. Gao X. Fire for hominin survivals in prehistory. Acta Anthropologica Sinica. 2020;39:333–48 (**in Chinese**).
28. Jordanova N, Petrovsky E, Kovacheva M, Jordanova D. Factors determining magnetic enhancement of burnt clay from archaeological sites. J Archaeol Sci. 2001;28:1137–48.
29. Hu YF, Zhou B, Peng Y, Xu XY. A review of study methods and progress on hominid use of fire. Quat Sci. 2019;29:240–57 (**in Chinese**).
30. Singh J, Sangode SJ, Sabale PD. Mineral magnetic and XRD spectroscopic studies to investigate the firing temperatures of archaeological potsherds. J Archaeol Sci: Rep. 2021;35: 102759.
31. Carrancho Á, Villalaín JJ, Angelucci DE, Dekkers MJ. Rock-magnetic analyses as a tool to investigate archaeological fired sediments: a case study of Mirador cave (Sierra de Atapuerca, Spain). Geophys J Int. 2009;179:79–96.
32. Zhang Y, Guo ZT, Deng CL, Zhang SQ, Wu HB, Zhang CX, et al. The use of fire at Zhoukoudian: evidence from magnetic susceptibility and color measurements. Chin Sci Bull. 2014;59:679–86 (**in Chinese**).
33. Jordanova N, Jordanova D, Barrón V, Lesigyarski D, Kostadinova-Avramova M. Rock-magnetic and color characteristics of archaeological samples from burnt clay from destructions and ceramics in relation to their firing temperature. Archaeol Anthropol Sci. 2019;11:3595–612.
34. Liu YT, Wang Y, Flad R, Lei XS. Animal sacrifice in burial: Materials from China during the Shang and Western Zhou period. Archaeol Res Asia. 2020;22:1–13.
35. Shi JS. Reconsidering of the Sanxingdui culture. Sichuan Cultural Relics. 2017;194:39–43 (**(in Chinese)**).
36. Sun H. Preliminary research on Sanxingdui Site. Southern Ethnol Archaeol. 2017;2:131–70 (**in Chinese**).
37. Zhang YH, Yang Y, Xian WK. Assessment to the geo-environmental status and problem prevention of Sanxingdui Ruins. Sichuan Cult Relics. 2005;1:21–8 (**in Chinese**).
38. Liu XS. The rise and fall of ancient cities in Chengdu Plain and the problem of ancient climate. Sichuan Cult Relics. 1998;4:34–7 (**in Chinese**).
39. Liu XS. Civilization and ancient geographic environment of Sanxingdui. J Chengdu Univ Technol. 2005;1:1–6 (**in Chinese**).
40. Liang B, Zhu B, Wang QW, Fu XF, Hao XF. Quaternary geology and environment of Chengdu Plain. Beijing: Science Press; 2014. (**in Chinese**).
41. Xie ZB, Xu DY, Han Y, Qiao G, Fu Y, Wang R, Xiang H, Li RL, Ran HL. 14C chronological study of No. 4 burial pit at the Sanxingdui Site, Guanghan, Sichuan. Sichuan Cult Relics. 2021;2:117–20 (**in Chinese**).
42. Sun H, Peng SY. New discoveries and new understandings of Sanxingdui burial pits. J Chinese Cult. 2022;6:95–116 (**in Chinese**).
43. Sun H. Bronze sets from Sanxingdui burial pits: Sacred offerings in the Sanxingdui temple to communicate with the deities. J Natl Museum China. 2023;9:42–55 (**in Chinese**).
44. Bagley R. Ancient Sichuan: treasures from a lost civilization. Princeton: Princeton University Press; 2001.
45. Carrancho Á, Villalaín JJ. Different mechanisms of magnetization recorded in experimental fires: archaeomagnetic implications. Earth Planet Sci Lett. 2011;312:176–87.
46. Li SP. Comparative research of magnetic susceptibility measurement in borehole and rock (core) susceptibility measurement. Contributions Geol Miner Resourc Res. 2018;33(02):282–5 (**in Chinese**).
47. Yin YG, Jia RX, Fang WX, Li SG, Qi YH, Zhang K, Li PG. Extraction of deep comprehensive information and its indicative significance of the Geriletu copper lead zinc polymetallic deposit in Ejina Banner, inner Mongolia. Miner Explor. 2023;14(8):1421–31 (**(in Chinese)**).
48. Scheinost AC, Schwertmann U. Color indetification of iron oxides and hydroxysulfates: use and limitations. Soil Sci Soc Am J. 1999;63:1463–71.
49. Robertson AR. The CIE 1976 color-difference formulae. Color Res Appl. 1997;2:7–11.
50. Gunal H, Ersahin S, Yetgin B, Kutlu K. Use of chromameter-measured color parameters in estimating color-related soil variables. Commun Soil Sci Plant Anal. 2008;39:726–40.
51. Zha LS, Wu KJ, Liang SY, Wei HB, Li CX. Indicative characteristics of soil in ancient human cultural sites-A case study of Yangshao Village Cultural Relics, Henan Province. Acta Pedol Sin. 2017;54:23–35 (**in Chinese**).
52. He KY, Tang M. Research on formation of the Baodun cultural cluster. J Chin Cult. 2020;3:71–82 (**in Chinese**).
53. Wang SR, Xu GR. Dual wavelength spectrophotometry. Jinan: Shandong Science and Technology Press; 1986. (**in Chinese**).
54. Hu CY, Huang JH, Fang NQ, Yang GQ. Stalagmites from Zha Cave, Qingjiang, Hubei Province: double wavelength reflectance spectrums and their paleoclimatic significance. Quat Sci. 2002;22:468–73 (**in Chinese**).
55. Hu ZY, Qin RB, Fan RW, Wang MY, Hu CY. The paleo-temperature significance of color of annual laminae stalagmite from Heshang cave, Central China. Quat Sci. 2018;38:1487–93 (**in Chinese**).
56. Le Borgne E. Susceptibilité magnétique anormale du sol superficiel. Ann Geophy. 1955;11:399–419.
57. Le Borgne E. Influence du feu sur les propriétés magnétiques du sol et sur celles du schiste et du granite. Ann Geophys. 1960;16:159–95.
58. Maher BA. Magnetic properties of some synthetic sub-micron magnetites. Geophys J. 1988;94:83–96.
59. Thompson R, Oldfield F. Environmental magnetism. London: Allen & Unwin Press; 1986.
60. Evans ME, Heller F. Environmental magnetism: Principles and applications of enviromagnetics. London: Academic; 2003.
61. Dearing JA. Magnetic susceptibility. In: Environmental Magnetism: A Practical Guide, No. 6. London: Quaternary Research Association; 1999. p. 35–62.
62. Bloemendal J, King JW, Hall FR, Doh SJ. Rock magnetism of Late Neogene and Pleistocene deep-sea sediments: relationship to sediment source, diagenetic processes, and sediment lithology. J Geophys Res. 1992;97:4361–75.
63. Li SY, Wang QH, Li BF, Gao F. Comparative study on the flammability of fresh leaves and living branches of 10 tree species in central Yunnan Province. J Southwest For Coll. 2006;1:56–8 (**in Chinese**).
64. Maezumi SY, Gosling WD, Kirschner J, Chevalier M, Cornelissen HL, Heinecke T, Mcmichael CNH. A modern analogue matching approach to characterize fire temperatures and plant species from charcoal. Palaeogeogr Palaeoclimatol Palaeoecol. 2021;578: 110580.
65. Zhu C, Xu JJ, Jia TJ, Zeng MX, Huang M. Environmental archaeology of the Rise and Fall of Sanxingdui and Jinsha Civilizations in Sichuan. Nanjing: Nanjing University Press; 2021. (**in Chinese**).
66. Wang QH, Zhao FJ, Xiao HJ, Li SY, Liu SY, Yang X. Simulation on fire behaviors of lithocarpus mairei shrubs in large forest fire sites in Anning. Yunnan J Shenyang Agric Univ. 2015;46:105–9 (**in Chinese**).
67. Zhang X, Wang J, Zhang WW, Wang QH, Long TT, Wang RC. Research progress of remote sensing technology for wildfire detection. J Shandong Forestry Sci Technol. 2022;52:117–22 (**in Chinese**).
68. Ding SC, Jiang CL. The narration and commentary of research on the ancient jade secondary alteration. Cult Relics Central China. 2012;6:36–44 (**in Chinese**).
69. Wang R, Zhu Y. Study progress on the whitening mechanism of ancient Chinese serpentine jade. Sci Conserv Archaeol. 2016;28:126–34 (**in Chinese**).

70. Sichuan Provincial Cultural Relics and Archeology Research Institute. Sanxingdui Sacrifice Pits. Beijing: Cultural Relic Publishing House; 1999. (**in Chinese**).
71. Ao TZ. Restudy of jade wares and stone artifacts in the Sanxingdui Site. Sichuan Cult Relics. 2003;2:39–45 (**in Chinese**).
72. Xu YJ, An Z, Huang N, Zhao DY. Analyzing the Shang-Western Zhou Dynasty pottery from the Jinsha Site with multi-technique method. Eur Phys J Plus. 2021;136:962.
73. Bellomo RV. A methodological approach for identifying archaeological evidence of fire resulting from human activities. J Archaeol Sci. 1993;20:525–53.
74. Scheffer F, Welte E, Ludwieg F. Zur frage der Eisenoxihydrate im Boden. Chem Erde-Geochem. 1957;19:51–64.
75. Mullins C. Magnetic susceptibility of the soil and its significance in soil science-a review. J Soil Sci. 1997;28:223–46.
76. Maher BA. Magnetic properties of modern soils and Quaternary loess paleosols: paleoclimatic implications. Palaeoecology. 1998;137:25–54.
77. Childs CW, Goodman BA, Churchman GJ. Application of Mössbauer spectroscopy to the study of iron oxides in some red and yellow/brown samples from New Zealand. Dev Sedimentol. 1979;27:555–65.
78. Torrent J, Schwertmann U, Fechter H, Alferez A. Quantitative relationships between soil color and hematite. Soil Sci. 1983;136:354–8.
79. Dunlop DJ, Özdemir Ö. Rock magnetism: fundamentals and frontiers. Cambridge: Cambridge University Press; 1997.
80. Liedgren L, Hörnberg G, Magnusson T, Östlund L. Heat impact and soil colors beneath hearths in northern Sweden. J Archaeol Sci. 2017;79:62–72.
81. Ulery AL, Graham RC. Forest fire effect on soil color and texture. Soil Sci Am J. 1993;57:135–40.
82. Sertsu SM, Sánchez PA. Effects of heating on some changes in soil properties in relation to an Ethiopian Land management practice. Soil Sci Soc Am J. 1978;42:940–4.
83. He L, Sun YB, An ZS. Changing color of Chinese loess: controlling factors and paleoclimatic significances. Geochimica. 2010;39:447–55 (**in Chinese**).
84. Cancelo-González J, Cachaldora C, Díaz-Fierros F, Prieto B. Colourimetric variations in burnt granitic forest soils in relation to fire severity. Ecol Indic. 2014;46:92–100.
85. Feng LW, Wu KN, Zha LS, Jü B, Wang WJ. Chroma characteristics and its climatic significance of Yangshao Culture Relic. Ecol Environ Sci. 2015;24:892–7 (**in Chinese**).
86. Tite MS, Mullins CE. Enhancement of the magnetic susceptibility of soil on archaeological sites. Archaeometry. 1971;13:209–19.
87. Shi W, Zhu C, Xu WF, Guan Y, Sun ZB. Relationship between abnormal phenomena of magnetic susceptibility curves of profiles and human activities at Zhongba Site in Chongqing. Acta Geogr Sin. 2007;62:257–67 (**(in Chinese)**).
88. Zhang GM, Xu LG, Zhang LL, Xu ZG. The excavation of the wooden frame sacrificial ware pit at the Shijia Site of Yueshi Culture, Huantai County, Shandong Province. Archaeology. 1997;11:1–18 (**in Chinese**).
89. Hu SZ. Buried sacrificial rituals-Inspiration from bronze statues and typical utensils of the Sanxingdui Site. Hohhot: 2012 China Art Anthropology Annual Conference and International Academic Seminar (Part III); 2012. p. 115–126 (in Chinese).
90. Zhou ZQ. Observations of the Ancient Shu people's sacrificial tradition in the sacrificial area of the Jinsha Site. Forum Chin Cult. 2019;5:16–22 (**in Chinese**).
91. Zhao DZ. Several Questions about the Sanxingdui Sacrificial Pit as the "Temple Fire Theory." Cult Relics Southern China. 2022;3:226–31 (**in Chinese**).
92. Fu S, Ye QP, Wang CS, Liu XS. On environmental evolution of disappearance of Sanxingdui civilization. Geol Sci Technol Inf. 2005;24(3):43–7 (**in Chinese**).
93. Xu PZ. Sichuan historical and archaeological collected works. Chengdu: Sichuan University Press; 2005. p. 6–10 (**in Chinese**).
94. Lin X. From Sanxingdui to Jinsha: searching for the lost Sanxingdui ancient city. Chin Lit Hist. 2006;8:122–7 (**in Chinese**).
95. Falkenhausen LV. The external connections of Sanxingdui. J East Asian Archaeol. 2003;5:191–245.
96. Zhou QH. On the cohesion and extrapolation of Bashu Culture from archaeological and documentary materials. Sichuan Cult Relics. 1993;1:7–12 (**in Chinese**).
97. Falkenhausen LV. The Chengdu plain in the early first Millennium BC: Zhuwajie. In: Bagley R, editor. Ancient Sichuan: treasures from a lost civilization. Princeton: Princeton University Press; 2001.
98. Falkenhausen LV. Les bronzes de Zhuwajie: une énigme archéologique. In Thote (ed.); 2003b. p. 195–203.
99. Fang YM, Liang FW. Preliminary study on WD2F1, building remains of venues for sacrificial rituals held in Longshan Culture Period, discovered at Wadian Site, Yuzhou Huaxia. Archaeolgy. 2021;6:62–75 (**(in Chinese)**).
100. Fu ZC. The cultural connection between Bashu and the southwestern barbarians. In: Li SM, Lin X, Xu NZ Eds. History, nationality, archaeology, and culture of two ancient states in modern Sichuan. Bashu Press; 1991 (in Chinese).
101. Wang ZN, Wang R. On the records of jade sacrifice liaoyu in oracle bone inscriptions. Cult Relics Central China. 2022;2:88–95 (**in Chinese**).
102. Pei MX. Discussion on Xiaoshuangqiao relics of early Shang Dynasty in Zhengzhou. Cult Relics of Central China. 1996;2:4–8 (**(in Chinese)**).
103. Song GD. A study of the sacrificial rituals in the middle Shang Dynasty-From the sacrificial remains of Xiaoshuangqiao Site in Zhengzhou. In: Study on Xia, Shang and Zhou Civilizations (Part VI). Anyang: International Symposium on Shang Civilization; 2004. pp. 427–433 (in Chinese).
104. Wang R, Wang CS, Tang JG. A jade parrot from the tomb of Fu Hao at Yinxu and Liao sacrifices of the Shang Dynasty. Antiquity. 2018;92(362):368–82.
105. Li AM. Study on the sacrificial content and custom reflected by the No. 1 and No. 2 buried pits of the Sanxingdui Site, Guanghan. Sichuan Cult Relics. 1994;4:5 (**in Chinese**).

Publisher's Note